Published in final edited form as:
Acta Biomater. 2015 February ; 13: 177–187. doi:10.1016/j.actbio.2014.11.015.

Click-coated, heparinized, decellularized vascular grafts

Sashka Dimitrievska[1], **Chao Cai**[2], **Amanda Weyers**[2], **Jenna L. Balestrini**[3], **Tylee Lin**[1], **Sumati Sundaram**[3], **Go Hatachi**[3], **David A. Spiegel**[4], **Themis R. Kyriakides**[1], **Jianjun Miao**[2], **Guoyun Li**[2], **Laura Niklason**[3], and **Robert J. Linhardt**[2]

[1]Department of Biomedical Engineering, Yale University, New Haven, CT 06510

[2]Department of Chemical and Biological Engineering, Rensselaer Polytechnic Institute, Troy, NY

[3]Department of Anesthesiology and Biomedical Engineering, Yale University, New Haven, CT 06510

[4]Departments of Chemistry and Pharmacology, Yale University, New Haven, CT 06510

Abstract

A novel method enabling the engineering of a dense and appropriately oriented heparin-containing layer on decellularized aortas has been developed. Amino groups of decellularized aortas were first modified to azido groups using 3-azidobenzoic acid. Azide-clickable dendrons were attached onto the azido groups through “alkyne-azide” click chemistry, affording a ten-fold amplification of adhesions sites. Dendron end groups were finally decorated with end-on modified heparin chains. Heparin chains were oriented like heparan sulfate groups on native endothelial cells surface. XPS, NMR, MS and FTIR were used to characterize the synthesis steps, building the final heparin layered coatings. Continuity of the heparin coating was verified using fluorescent microscopy and histological analysis. Efficacy of heparin linkage was demonstrated with factor Xa antithrombogenic assay and platelet adhesion studies. The results suggest that oriented heparin immobilization to decellularized aortas may improve the *in vivo* blood compatibility of decellularized aortas and vessels.

Introduction

Demand for non-thrombogenic arterial conduits persists due to the poor clinical performance of existing synthetic grafts for small-diameter artery applications. Decellularized native and tissue engineered vascular grafts (TEVGs) have shown success in large diameter vascular applications [1–4]. The decellularization process necessary for the removal of cellular antigens also removes the endothelial cells (ECs) lining the lumen that is responsible for inhibition of coagulation and platelet adhesion [5]. Following the removal of ECs, the damaged vascular wall contains exposed collagen, a highly thrombogenic surface, which in small-diameter vascular grafts activates platelets and blood coagulation proteins [6]. Thus,

one potential solution to preventing thrombus formation, subsequent occlusion, and graft failure is to modify the decellularized vascular surfaces by "hiding" the exposed thrombogenic collagen with non-thrombogenic chemical structures such as heparan sulfate [7,8].

To avoid thrombogenic failure, the common approach used by others in the past has been the linking of heparin to decellularized grafts. Typically, heparin is linked to the extracellular matrix (ECM) using a "one-to-one" (one active group of ECM-to-one heparin chain) crosslinker such as glutaraldehyde [9] and 1-(3-dimethylaminopropyl)-3-ethylcarbodiimide hydrochloride (EDC) [10–12]. As there are few surface accessible amino groups on the ECM, the "one-to-one" approach results in a low surface coverage of heparin. In addition, heparin's anticoagulant efficacy depends on its ability to bind antithrombin III (ATIII) through the appropriate presentation of its ATIII-specific pentasaccaride sequence [13]. Lack of control over the heparin orientation, in combination with low amounts of heparin attachment, have been the main reasons for limited success following chemical immobilization of heparin on vascular grafts. These issues have been somewhat addressed on polymeric grafts, where the surface modification methodologies are more numerous, with end-grafted heparin layers currently being clinically favored [7,14–16]. As an example of heparin coated vascular grafts, Gore's end-on heparin coated Dacron grafts Propaten® demonstrated in a femoroepoplitaeal bypass clinical study a 17% increase in first-year patency values, as compared to untreated polytetra-fluoroethylene (PTFE) grafts [17]. However, the primary patency rate of Propaten® grafts at 48 months was 17.2% lower than in ipsilateral autologous saphenous vein (the industry gold standard) [18].

While directional coupling chemistry has been used to immobilize heparin to polymeric structures such as PTFE[19] and nanomaterials [2–23], it has not been previously reported on dendrons/dendrimers or on biological structures. Here we present a novel method that enables the synthetic engineering of a dense, oriented heparin-containing layer on biological structures, such as decellularized vessels. We are able to recreate the dense packing and relevant structural orientation by first amplifying the existing labile chemical groups using azide-clickable dendrons, and then decorating the surface of the dendrons with end-on oriented heparin, which mimics the orientation of heparan sulfate on the EC surface.

Materials and methods

Materials

Polyester-8-hydroxyl-1-acetylene bis-MPA dendron, 3-mercaptopropionic acid, 3-aminobenzoic acid, trityl chloride (TrCl), adipic acid dihydrazide (ADH), generation 3, 1-ethyl-3-(3-dimethylaminopropyl)carbodiimide hydrochloride (EDC), N-hydroxysuccinimide (NHS), 4-dimethylaminopyridine (DMAP), 2-morpholinoethane sulfonic acid (MES), trypsin, (3-[(3-Cholamidopropyl)dimethylammonio]-1-propanesulfonate (CHAPS), phosphate-buffered saline (PBS), sodium cyanoborohydride ($NaBH_3CN$), Sodium Chloride (NaCl), general solvents and reagents were purchased from Sigma. Sulfosuccinimidyl 4-[N-maleimidomethyl]cyclohexane-1-carboxylate (Sulfo-SMCC) was purchased from Thermo Fisher Scientific Inc. Fetal bovine serum (FBS) was purchased from Gibco. Factor Xa (FXa) and ATIII were purchased from Sigma.

Preparation of decellularized aortic tissues

Fresh porcine descending abdominal aortas (inner lumen diameter around 2 cm) were harvested from a local slaughterhouse and transported on ice to the lab. Immediately after arrival, the aortas were cleaned of adherent tissues and fat, and rinsed in phosphate buffered saline (PBS). The aortas were decellularized by first incubating them in a solution of: 8 mM 3-[(3-Cholamidopropyl)dimethylammonio]-1-propanesulfonate hydrate (CHAPS), 1 M NaCl, and 25 mM EDTA in PBS for 24 h on a stir plate at 37 °C. Aortas were then washed three times in PBS for 10 min, followed by an overnight rinse in 10% fetal bovine serum (FBS) in PBS for 24 h on a stir plate at 37 °C. After the decellularization process, using a sterilized cutting tool aortas were cut into 1-cm circular shaped discs. To verify the removal of all cellular materials, the aortas were fixed in neutral-buffered formalin, and stained with hematoxylin and eosin (H&E) to identify nuclear material. To evaluate the decellularization quantitatively, the DNA content of fresh and decellularized porcine aortas was determined using the PicoGreen assay. Briefly, aortas segments were lyophilized, weighed, and digested in papain buffer (papain 125 μg/mL (Sigma, Saint Louis, MO), 5 mM cysteine-HCl, and 5 mM di-sodium EDTA in PBS) at 60° C overnight. The papain sample solution was diluted with buffer (10 mM Tris-HCl and 1 mM EDTA, pH 7.5; Invitrogen), incubated with an equal volume of Quant-iT™ PicoGreen® dsDNA reagent (Molecular Probes, Eugene, OR), and using a fluorometer, the fluorescence was measured at an excitation wavelength of 485 nm and an emission wavelength of 530 nm. The complete decellularization of the aortas was also confirmed using β-actin immunoblotting. Proteins were extracted from homogenized frozen fresh and decellularized porcine aortas tissue samples in lysis buffer (50 mM Tris-HCl, pH 7.4, 150 mM NaCl, 1% [v/v] Triton X-100, 0.5% [w/v] sodium deoxycholate, and 0.1% [w/v] SDS) containing freshly added proteinase inhibitors (Sigma-Aldrich, St. Louis, MO). The protein concentration was determined using the Bradford protein assay (Bio-Rad Laboratories, Hercules, CA). Samples were prepared for SDS-Polyacrylamide gel electrophoresis (PAGE) by boiling 30 μg of proteins in SDS sample buffer containing 2% β-mercaptoethanol (final concentration) for 5 min. SDS-PAGE and immunoblotting was performed similarly as previously described. Briefly, proteins were separated by electrophoresis, transferred to polyvinylidene difluoride (PVDF) membrane (Bio-Rad), and immunoblotted with mouse monoclonal antibody to β-actin (1:2500; Sigma-Aldrich), followed by horseradish peroxidase–conjugated goat anti-mouse secondary antibody. Blots were developed using enhanced chemiluminescence (Pierce Biotechnology, Rockford, IL). The DNA content and β-actin immunoblots are shown in supplementary Figure 1. The absence of H&E cellular nuclei staining was taken as indicative of complete decellularization of the aortas. Aorta pieces were then snap frozen at −80 °C and sliced to 35 μm thickness using a cryostat without using mounting medium, to preserve the native decellularized chemistry of the aortic luminal surfaces.

Synthesis of maleic attached heparin

Sulfhydryl-reactive end-on modified heparin was produced by end-on modifying heparin with maleimide as illustrated in Figure 1 panel A. Briefly, heparin (100 mg, 8.3 μmol) was added into 10 mL of heated formamide followed by the addition of dissolved adipic acid dihydrazide (ADH) (100 mg, 920 μmol) and maintained at 50 °C for 6 h. Aqueous sodium cyanoborohydride (9.5 mg, 150 μmol) was added and incubated at 65 °C for an additional 24

h. The reaction mixture was diluted with 50 mL of water and dialyzed against 2 L of water for 48 h using a 3500 molecular weight cutoff (MWCO) dialysis membrane. The retentate was recovered, lyophilized, and purified by ethanol precipitation to obtain the ADH-heparin derivative (Figure 1, compound **2**). Sulfo-SMCC (23 mg, 50 μmol) was added to the ADH-heparin derivative (75 mg, 5 μmol) in PBS buffer, and the solution was incubated for 2 h. Unreacted maleimide groups of sulfo-SMCC were quenched by aqueous solution of mercaptoethanol (1 mmol). The reaction solution was diluted with 10 mL of water and dialyzed against 2 L of water for 48 h using a 3500 MWCO dialysis membrane. The retentate was recovered, lyophilized, and purified by ethanol precipitation to obtain the maleic-heparin derivative. The resulting compound of this three-step modification is identified in Figure 1A as compound **3**.

Synthesis of heparin-modified dendron coatings of decellularized aortas by click chemistry

Pre-activated 3-azidobenzoic acid was used to modify the exposed primary amines of the decellularized aortas to azide groups. 3-Aminobenzoic acid (**4**) was converted to the corresponding azide (**5**) upon treatment with sodium azide and sodium nitrate under acidic conditions (Figure 1B). Compound **5** (25 mg, 0.07 mmol) was then dissolved in N, N'-dimethylformamide (DMF, 1 mL), added to a solution of 1-ethyl-3-[3-dimethylaminopropyl] carbodiimide hydrochloride (EDC) (19.2 mg, 0.10 mmol), and allowed to stir for 15 min at room temperature. Decellularized aortas (**10**) were then treated with this solution, and allowed to incubate for 12 h at room temperature to afford azide-functionalized vascular grafts (**11**). Presumably, covalent attachment of **5** to decellularized aortas is mediated by acylation of the amino groups in collagen (Figure 1E, compound **11**).

Immobilization of dendrons on the azido-modified decellularized aortas was then achieved by "alkyne-azide" click chemistry [24]. Thus, dendron **9** (14 mg, 7.88 μmol) and L-ascorbic acid (2.8 mg, 15.7 μmol) were dissolved in DMF (1 mL), added to the azide-containing decellularized aorta, then exposed to $CuSO_4$ (0.1 M in PBS solvent, 10 mL). The reaction mixture was gently shaken at room temperature for 6 h to afford **12** (Figure 1E).

Dendrons were next deprotected at room temperature with 50% trifluoroacetic acid (TFA), and rinsed with water to reveal free thiol-groups. Exposure of the resulting material to maleimide-modified heparin (**3** mL of a 10 mM solution in PBS) under argon atmosphere, followed by repeated washing with PBS to stop the coupling reaction, provided conjugate **13** (Figure 1E).

Characterization of heparin-modified dendron coatings on decellularized aortas

FTIR spectroscopy was conducted using a Perkin-Elmer Spectrum One Fourier Transform Infrared Spectrometer. The solid samples were first mixed with KBr and ground to a fine powder by using a mortar and pestle. Then they were pressed into pellets under compression pressure of 2000 kg/cm^2 for 30 s. Sample spectra were obtained using an average 32 scans over the range between 800 and 4000 cm^{-1} with a spectral resolution of 2 cm^{-1}.

X-Ray Photoelectron Spectroscopy (XPS) experiments were operated in an ultra high vacuum chamber using a hemispherical electron energy analyser (HA100, VSW Ltd., UK) and a monochromatized Al X-ray source. The spectra were collected at a take-off angle of 45°. Survey spectra were acquired with a pass energy of 117.4 eV. The binding energy scale was calibrated using the aliphatic component of the C 1s peak as 285.0 eV.

Liquid chromatography mass spectrometry (LC-MS) combined with disaccharide compositional analysis, were used to quantify the heparin content of decellularized aortas. Briefly, a mixture of heparinase I, II, and III (5 milli-unit each) was added to the coated decellularized aortas and incubated overnight at 37 °C. Heparin disaccharides were recovered by centrifugal filtration using an YM-10 spin column and lyophilized overnight. Heparin/heparan sulfate disaccharide standards had the following structures: ΔUA(1→4)GlcNAc (0S), ΔUA2S(1→4)GlcNAc (2S), ΔUA(1→4)GlcNcA6S (6S), ΔUA2S(1→4)GlcNAc6S (2S6S), ΔUA(1→4)GlcNS (NS), ΔUA2S(1→4)GlcNS (NS2S), ΔUA(1→4)GlcNS6S (NS6S) and ΔUA2S(1→4)GlcNS6S (TriS), where ΔUA is 4-deoxy-α-L-*threo*-lex-4-enopyranosyluronic acid, GlcN is glucosamine, S is sulfo, and Ac is acetyl. All disaccharide standards were from Iduron Ltd. (Manchester, United Kingdom). Unsaturated disaccharides were then labeled using 2-aminoacridine (AMAC) by adding 10 μl of 0.1 M AMAC solution onto heparin-derived disaccharides (~5 μg) or a mixture of 8 heparin disaccharide standards (5 μg/ disaccharide). Next, 10 μL of 1 M $NaBH_3CN$ was added in the reaction mixture and incubated at 45 °C for 4 h. Finally, the AMAC-tagged disaccharides were diluted to different concentrations (0.5–100 ng) using 50% (v/v) aqueous DMSO. LC-MS analyses were performed on an Agilent 1200 LC/MSD instrument (Agilent Technologies, Inc. Wilmington, DE) equipped with a 6300 ion-trap and a binary pump. A Poroshell 120 C18 column (3.0 × 150 mm, 2.7 μm, Agilent, USA) at 45 °C was used. Eluent A was 80 mM ammonium acetate and eluent B was methanol. Solution A and 15% solution B was flowed (150 μl/min) through the column for 5 min followed by linear gradients 15–30% solution B from 5 to 30 min. The electrospray interface was set in negative ionization mode with a skimmer potential of - 40.0V, a capillary exit of 40V, and a source temperature of 350 °C, to obtain the maximum abundance of the ions in a full-scan spectrum (300–1200 Da). Nitrogen (8 L/min, 40 psi) was used as a drying and nebulizing gas.

Functional analysis of heparin in “click” synthesized coatings of decellularized aortas

Amount of functionally bound heparin on the decellularized aortas was determined using the FXa assay. This method is based on the conformational change of the serine proteinase inhibitor ATIII by heparin, resulting in FXa inhibition. Capacity of aorta-bound heparin to inhibit the blood coagulation cascade was assessed by incubating the decellularized aortas with 100 μL ATIII (25 mU) in 50 mM Tris buffer (pH 8.4) for 5 min at 37 °C under constant agitation to allow ATIII to bind to heparin. Heparin standards (0–100 ng dissolved in 50 mM TRIS, 7.5 mM Na_2EDTA, 175 mM NaCl buffer) were used as controls. FXa (20 U/mL in 1 mg/mL BSA/PBS) was added and incubated for 2 min at 37 °C to allow activated ATIII to inactivate FXa. Supernatants were then transferred into a 96-well plate, 25 μL of 1 mM chromogenic substrate S-2222 (Chromogenix) was added, and the mixture was stirred for 10 min at 37 °C, allowing the remaining active FXa to hydrolyze the substrate, thereby

releasing chromophore *p*-nitroaniline. Absorbance readings were taken every minute for the 10 min duration of the reaction.

Imaging of "Click" coating

Histological analysis: decellularized aortas (control samples) and "click" heparin coated decellularized aortas samples were fixed in 10% (v/v) neutral-buffered formalin for 1 h, embedded in paraffin, cut into 5-μm sections, and stained with GAG binding dies: alcian blue, toluidine blue and combined alcian blue-periodic acid schiff (PAS) stain. Images were obtained using an Axiovert 200M microscope (Zeiss, Thornwood, NY) equipped with AxioCam HR with software AxioVision Release 4.5.

Confocal microscopy: coated decellularized aortas were visualized by confocal microscopy by incubating the samples at room temperature for 1 h with ATIII at 1 unit/mL labeled with fluorescein isothiocyanate (FITC) or FITC-labeled wheat germ agglutinin antibody. Images were acquired with a confocal microscope (Zeiss LSM 510 Meta; Carl Zeiss, Jena, Germany) equipped with an Axiovert 200 microscope. Z-stacks were acquired using the 488-nm laser line, a 40X objective, and three-dimensional projections of the acquired z-stacks were analyzed using Leica software.

Transmission electron microscopy (TEM) analysis: decellularized aortas (control samples) and "click" heparin coated decellularized aortas were fixed for 1 h in 2.0% paraformaldehyde and 2.5% glutaraldehyde containing 0.075% ruthenium red, 75 mM lysine, and 0.1 M cacodylate at pH 7.2 and then fixed in the same solution with lysine removed. (The ruthenium red component of the fixative solution binds to the negatively charged heparin chains of the coating.) Following a rinse with 0.1 M cacodylate alone, collagen scaffolds were post-fixed with 1% osmium tetroxide to enhance contrast between the coating and collagen and dehydrated through a graded series of ethanol solutions, and embedded in LX112 Resin.

Platelet adhesion on click-coated grafts

To isolate platelets, whole blood from Sprague Dawley rat hearts was drawn into a syringe containing 3.8% sodium citrate (volume ratio blood: sodium citrate 9:1). Whole blood was then centrifuged at 200 *g* for 10 min at 22 °C to isolate the platelet-rich plasma (PRP). Decellularized aortas were cut to fit into a 24-well plate and 200 μL of PRP was incubated for 30 min at 37 °C. To fix the adhered platelets, the samples were rinsed three times in PBS (5 min each) and then fixed in 4% glutaraldehyde for 24 h, washed in phosphate-buffered saline three times, and dehydrated using graded ethanol. Next, the specimens were dried in a vacuum dryer, sputter-coated with carbon, and observed using scanning electron microscopy (SEM).

Endothelial cell adhesion on click-coated grafts

To investigate the cell attachment in the initial period, and the "click" coating support of cell proliferation decellularized "click" coated and untreated aortas were cut to fit into a 24-well plate. Human Umbilical Vein Endothelial Cells (HUVECs) were isolated from umbilical veins by treatment with collagenase and serially passaged 2–6 times in gelatin-coated tissue

culture plastic using M199 medium supplemented with 20% FBS, 2% L-glutamine, 1% penicillin, and streptomycin and endothelial cell growth supplement [*i.e.*, fibroblast growth factor 1 (FGF-1), 1:100 dilution; BD Biosciences, San Jose, CA, USA] at 37°C in a 5% CO_2 humidified air incubator. Decellularized "click" coated and untreated aortas were seeded with 100 μl of 5×10^5 HUVECs. At identified time-points the non-adherent cells were rinsed with PBS washes from the cell-seeded grafts prior to fixation and visual analysis. The adherent cells on the grafts were fixed with 4% paraformaldehyde (PFA) for 15 min, permeabilized with 0.5% (v/v) Triton-X 100 (Sigma, USA) for 10 min and blocked with 5% (v/v) bovine serum albumin (BSA) (Sigma, USA). Finally, cells bodies were stained with Rhodamine-phalloidin (Sigma, USA) and cell nuclei with 4, 6-diamidino-2-phenylindole (DAPI) (1 μg/ml) for 30 min. Cell-seeded grafts were mounted in Vectashield and examined using a Leica TCS SP5 spectral confocal microscope (Leica Microsystems, Bannockburn, IL, USA).

Tensile testing

Decellularized aortas (control samples) and "click" heparin coated decellularized aortas samples were cut into 10 mm × 2 mm × 65 mm (length × width × thickness) strips for mechanical analysis using an Instron 5848. Care was taken to ensure sample integrity prior to analysis. Tissue length and width of each sample was determined by a series of measurements at four different points using a Mitutoyo digital micrometer. Specimens were glued to 1 mm sections of sand paper at each end of the tissue slices, and each end was affixed to grips. Tissues were then cyclically preconditioned for 3 cycles to 15% strain, and pulled until failure at a strain rate of 1%/sec. The axial force was measured with a 10 N load cell, and elongation assessed by cross-head displacement. Tissues were kept hydrated with PBS before and during the mechanical conditioning. Using tissue dimensions, engineering stress and strain were calculated from force and distance from the slope at the linear regions of the curve using the equations 1.1–[1.2]:

$$\sigma = \frac{F}{A_0} \text{ where } \sigma \text{ is engineering stress, F = Force, and } A_0 \text{ = initial area} \quad (1.1)$$

$$\varepsilon = \frac{l_f - l_o}{l_o} \text{ where } \varepsilon \text{ = engineering strain, } l_f \text{ = final length, } l_0 \text{ = initial length} \quad (1.2)$$

The Young's Modulus (E) for the tissue was determined by dividing the engineering stress, σ, by the engineering strain ε.

Disclaimer:
L.E.N. has a financial interest in Humacyte, Inc, a regenerative medicine company. Humacyte did not fund these studies, and Humacyte did not affect the design, interpretation, or reporting of any of the experiments herein.

Results and discussion

Synthesis and characterization of “click” coated surface

Our strategy for coating decellularized aortas consisted of four parts. The first step was to convert surface-exposed amino groups on decellularized aortas into azido groups (Figure 1E, compound **11**) [25]. As a second step we anchored the polyester-8-hydroxyl-1-acetylene bis-MPA dendron (Figure 1E, compound **12**) [26], which creates eight new attachment sites for every modified amine, and extends the dendron’s end groups toward the luminal side of the vessel. The third step is performed away from the vessel and consists of the conversion of the hydroxyl end groups of the dendron core (**8**) into thio-trityl leaving groups (Figure 1D, compound **9**), which was verified by NMR (Figure S4) and HR-MS (Figure 2). In ^{1}H NMR spectroscopy of **9**, the terminal proton on alkyne group of dendron is identified at 2.46 ppm (J = 2.52 Hz), which confirms that the triple bond is at the end of a chain as well (Figure 2). Newly generated proton peaks between 7.0 and 7.5 ppm corresponding to aromatic protons show the successful attachment of trityl-protected linker. Multiple peaks in HR-MS spectroscopy set for the different adducts of dendritic molecule including $[M+2NH_4]^{2+}$, $[M+NH_4+Na]^{2+}$ and $[M+2Na]^{2+}$.

The 8 available end groups were next modified by attaching heparin “end-on” onto the dendron end-groups (Figure 1, compound **13**). “End-on” heparin attachment allows the ATIII-binding pentasaccharide sequence within the heparin chain to remain exposed and accessible. The anomeric position of the terminal sugar in each heparin chain (Figure 1, compound **1**) can be reductively aminated with adipic acid dihydrazide (ADH) to afford a conjugate structure (**2**). The second hydrazide group of ADH is then coupled to sulfo-SMCC to introduce a maleimide functional group (**3**). Terminally-modified heparin derivative functionally preserves the ATIII-binding pentasaccharide sequences within the heparin chains. Heparin derivatives **1**–**3** were characterized using ^{1}H-NMR spectroscopy [27].

^{1}H-NMR spectra corresponding to heparin derivatives **1**–**3** are shown in Figure 3. ^{1}H-NMR characterization of ADH-maleimide displayed the maleimide double bond as a single peak at 6.75 ppm, as well as two broad peaks at 1.60 ppm and 2.30 ppm belonging to the 8 protons on the ADH (Figure 3, green spectrum identified by green dashed box). In the ^{1}H-NMR, typical proton peaks at 6.75, 1.60 and 2.30 ppm appear together, and the ADH-modified heparin **2** (Figure 3, red spectrum) lacks the 6.75-ppm maleimide-specific peaks, confirming the successful addition of ADH and maleimide respectively.

Maleimide-modified heparin chains were then linked “end-on” onto the exposed thiol residues of the dendrons’ 8 end groups (Scheme S1, compound **S12**). Covalently linked dendrons containing heparin on the decellularized aortas (**13**) were characterized using XPS and FTIR (Figure 4). XPS scans of the S2p peaks at 168eV shown as overlaid decellularized aortas (**10**), dendron-heparin coated decellularized aortas (**13**) and heparin derivative (**3**) demonstrate a sharp intensity increase on the dendron-heparin coated decellularized aortas. The S2p peak (168eV) intensity increase is indicative of the successful immobilization of sulfated heparin as a result of the heparin layer addition (Figure 4A). Furthermore, the FTIR spectrum of overlaid decellularized aortas (**10**), dendron-heparin coated decellularized aortas (**13**) and heparin derivative (**3**) (Figure 4B), also demonstrates an increase in the peaks

intensity at 1015 cm^{-1}, which is a region assigned to sulfate group vibrations [27]. The FTIR peaks increase at 1015 cm^{-1} also confirms the addition of heparin content on the decellularized aorta, indicating successful attachment of the dendrons and heparin layers.

Initial surface analysis experiments confirmed the individual end-on heparin and dendron modifications on decellularized aortas. In addition to this first part, the heparin modification allowing for the end-on oriented addition leading to reduced steric interference and exposed ATIII binding sites [28] was confirmed through ^{1}H-NMR identification of signals corresponding to maleimide and ADH. Modification of the dendrons hydroxyl groups into trityl leaving groups was confirmed using ^{1}H-NMR. “Click” attachment of the dendrons and heparin onto decellularized aortas was confirmed using FTIR and XPS, via the presence of sulfate groups.

Heparin quantification and functionality

We next verified the capacity of the attached heparin on the decellularized aortas to inactivate the coagulation cascade (biofunctionality) as a percentage of the total amount of attached heparin. Total heparin quantification was performed by cleaving the covalently linked heparin from the modified decellularized aortas, using a mixture of heparin lyases I, II, and III. Released heparin disaccharides were then quantified by LC-MS. Extracted ion chromatogram (EIC) of the disaccharide analysis is presented in Figure 5A. Eight common heparin disaccharides were detected in the heparin-coated decellularized aorta, and the amounts of each were calculated from a calibration curve of disaccharide standards. The major disaccharide in heparin-coated decellularized aorta was trisulfated disaccharide (TriS), comprising 68.18% of the total heparin content. By summing all the released disaccharides, it was determined that covalently-linked heparin was deposited at a density of 16 μg per cm^2 of decellularized aortas.

Next, to ascertain the functional activity of covalently-linked heparin, we measured the ability of surface-bound heparin to inactivate FXa using an anti-FXa activity assay. This assay determines the ability of the functionalized surface to bind the serine protease inhibitor ATIII, resulting in ATIII conformational activation, and leading to the inhibition of FXa. The amount of surface-bound heparin was estimated based on the effect of solution heparin at a known concentration (Figure 6). Heparin-coated on the decellularized aorta per cm^2 inactivated FXa corresponding to 10 μg of heparin in solution. Comparison to the disaccharide analysis data of 16 μg per cm^2, demonstrated that 80% of the total surface bound heparin retained functional activity for binding and activating ATIII and inhibiting FXa. While the FXa assay only represents a portion of the entire coagulation cascade, it seems reasonable to suggest that the surface bioactivity of the covalently linked heparin has been largely retained using our coupling chemistry. This comparison provides only an estimate, as it also fails to take into account the differences in heparin activity when heparin is in solution versus when heparin is covalently attached to a surface.

In conclusion the heparin covalently immobilized to the decellularized aorta was quantified 0.016 mg/cm^2 using LC-MS. This immobilized heparin is functionally equivalent to 0.01 mg heparin in solution in the inactivation of FXa, corresponding to ~80% of functionally

deposited heparin per cm^2, which we speculate should be sufficient to maintain blood fluidity through the decellularized aorta.

Visualization of functional components of coating

We performed a series of histology and microscopy studies to further document the presence and uniformity of the heparin coating. Spatial uniformity of the immobilized heparin is critically important since a “patchy” coating would expose underlining decellularized aorta collagen, leading to thrombogenic sites. Histochemical dyes that bind to GAGs were used to assess the continuity of the coating. Alcian blue binds to sulfated polysaccharides and toluidine blue binds to negatively charged moieties. Both histochemical dyes demonstrate a continuous layer of heparin over the surface of the decellularized aortas (Figure 7, images C and D). In comparison, the controldecellularized aorta only demonstrates a background absorbance color thought the graft matrix (Figure 7, images A and B).

We next fluorescently labeled ATIII with FITC (ATIII-FITC), and probed for heparin chains that can bind to and retain ATIII to further assess the functionality of the surface-bound heparin. ATIII-FITC revealed a continuous fluorescent layer on coated decellularized aortas (Figure 8). In addition, the coating visualized by ATIII-FITC was similar to wheat germ agglutinin antibody staining, which binds *N*-acetyl-D-glucosaminyl residues, a constituent of heparin [29].

To gain a better understanding of the coating on an ultrastructural level, the vessel surfaces were viewed under TEM. The control decellularized abdominal aorta reveals damaged elastin layer and luminally exposed collagen fibbers mostly transversally coming out of view plan. The elastin combination with exposed collagen create a highly thrombogenic surface. Following the “click” coating, the recreation of a luminal barrier of about 500 nm thick that continuously covers the exposed collagen fibers is clearly visible. This continuous barrier is structurally made up of the hyperbranched dendrons layered onto the anchor amine points. The heparin chains extending from the dendrons are also visible as fuzzy hair-like structures extending out of the coating surface luminally.

Platelet adhesion studies

Platelet adhesion and activation was evaluated pre-heparin and post-heparin immobilization using SEM imaging. Both the number of adhering platelets and their morphological appearance (typically identified by “pseudopods” when stretching out in activated states) are important to evaluate the blood compatibility of a surface. As reported by others, decellularized aortas allow a confluent layer of platelets to adhere to the surface due to the collagen fiber exposure. By SEM, we observed that freshly isolated platelets did indeed adhere to, and activated on, the uncoated decellularized aorta surface (Figure 10). However, post-heparin immobilization, the number of the adherent platelets substantially decreased to a level where they were difficult to detect. Few adherent platelets that were observed showed a rounded morphology, with very few pseudopodia and deformations. Low adsorption of platelets following heparin coating indicates that the blood compatibility of the decellularized aortas is highly improved.

"Click" coating effects on endothelial cell viability

The morphology of HUVECs after 1 and 7 days of incubation on "click" coated and control untreated grafts is shown in Figure 11. By visualization, both the initial adhesion (Day 1) and growth (Day 7) of the endothelial cells is at least as good on the "click" coated grafts as it is on the control grafts. There appears to be a higher number of cell bodies both at Day 1 and at Day 7 on the "click" coated grafts, indicating the "click" coating supports endothelial cell adhesion and proliferation.

"Click" coating effects on grafts mechanics

Results from mechanical testing of the decellularized untreated and "click" coated grafts are shown in Figure 12. "Click" coated grafts were slightly stiffer than decellularized controls (Young's modulus 1.69 ± 0.25 versus 1.48 ± 0.38 MPa), although this difference was not significant. These data suggest that at deformations of up to 25% strain, "click" coated tissue closely resembles control tissues in terms of stress-strain relationships. In terms of the tissue integrity post "click" coating, acellular tissue had a Young's moduli that resembled control grafts in low and large (~ 30%) deformation ranges.

Conclusion

A novel method for covalently linking oriented-heparin at high density to decellularized aortas was developed that relied on "alkyne-azide" clickable dendrons. Successful grafting of the azide groups onto decellularized aortas was verified through the use of ^{1}H-NMR on "clicked" dendrons. XPS and FTIR detection of the heparinspecific sulfate groups demonstrated the successful end-on heparin modification of the dendrons. Functionality of the oriented, covalently-linked heparin was demonstrated using the antithrombogenic FXa assay. Capacity of native endothelialized vessels to inactivate FXa, lost post-decellularization, was re-established following the immobilization of heparin to the decellularized aortas. Platelet adhesion assay also showed a substantial reduction following the heparin immobilization.

Supplementary Material

Refer to Web version on PubMed Central for supplementary material.

Acknowledgments

Grant support:

This work was supported by the Howard Hughes Medical Institute (fellowship to SD) and NIH R01 HL083895-01 (to LEN).

References

1. Dahl SL, Kypson AP, Lawson JH, Blum JL, Strader JT, Li Y, et al. Readily available tissue-engineered vascular grafts. Sci Transl Med. 2011; 3:68ra9.
2. Shin'oka T, Matsumura G, Hibino N, Naito Y, Watanabe M, Konuma T, et al. Midterm clinical result of tissue-engineered vascular autografts seeded with autologous bone marrow cells. J Thorac Cardiovasc Surg. 2005; 129:1330–1338. [PubMed: 15942574]

3. McAllister TN, Maruszewski M, Garrido SA, Wystrychowski W, Dusserre N, Marini A, et al. Effectiveness of haemodialysis access with an autologous tissue-engineered vascular graft: a multicentre cohort study. Lancet. 2009; 373:1440–1446. [PubMed: 19394535]

4. Niklason LE, Gao J, Abbott WM, Hirschi KK, Houser S, Marini R, et al. Functional arteries grown in vitro. Science (80-). 1999; 284:489–493.

5. Reitsma S, Slaaf DW, Vink H, van Zandvoort MA, oude Egbrink MG. The endothelial glycocalyx: composition, functions, and visualization. Pflugers Arch. 2007; 454:345–359. [PubMed: 17256154]

6. Saelman EU, Nieuwenhuis HK, Hese KM, de Groot PG, Heijnen HF, Sage EH, et al. Platelet adhesion to collagen types I through VIII under conditions of stasis and flow is mediated by GPIa/IIa (alpha 2 beta 1-integrin). Blood. 1994; 83:1244–1250. [PubMed: 8118028]

7. Gupta AS, Wang S, Link E, Anderson EH, Hofmann C, Lewandowski J, et al. Glycocalyx-mimetic dextran-modified poly(vinyl amine) surfactant coating reduces platelet adhesion on medical-grade polycarbonate surface. Biomaterials. 2006; 27:3084–3095. [PubMed: 16460796]

8. Holland NB, Qiu Y, Ruegsegger M, Marchant RE. Biomimetic engineering of non-adhesive glycocalyx-like surfaces using oligosaccharide surfactant polymers. Nature. 1998; 392:799–801. [PubMed: 9572137]

9. Lee WK, Park KD, Han DK, Suh H, Park JC, Kim YH. Heparinized bovine pericardium as a novel cardiovascular bioprosthesis. Biomaterials. 2000; 21:2323–2330. [PubMed: 11026639]

10. Liao D, Wang X, Lin PH, Yao Q, Chen CJ. Covalent linkage of heparin provides a stable anti-coagulation surface of decellularized porcine arteries. J Cell Mol Med. 2009; 13:2736–2743. [PubMed: 19040421]

11. Wissink MJ, Beernink R, Pieper JS, Poot AA, Engbers GH, Beugeling T, et al. Immobilization of heparin to EDC/NHS-crosslinked collagen. Characterization and in vitro evaluation. Biomaterials. 2001; 22:151–163. [PubMed: 11101159]

12. Yu S-H, Wu Y-B, Mi F-L, Shyu S-S. Polysaccharide-based artificial extracellular matrix: Preparation and characterization of three-dimensional, macroporous chitosan, and heparin composite scaffold. J Appl Polym Sci. 2008; 109:3639–3644.

13. Olson ST, Bjork I. Regulation of thrombin activity by antithrombin and heparin. Semin Thromb Hemost. 1994; 20:373–409. [PubMed: 7899869]

14. Hoffman J, Larm O, Scholander E. A new method for covalent coupling of heparin and other glycosaminoglycans to substances containing primary amino groups. Carbohydr Res. 1983; 117:328–331. [PubMed: 6883369]

15. Goosen MF, Sefton MV. Properties of a heparin-poly(vinyl alcohol) hydrogel coating. J Biomed Mater Res. 1983; 17:359–373. [PubMed: 6841373]

16. Sperling C, Fischer M, Maitz MF, Werner C. Blood coagulation on biomaterials requires the combination of distinct activation processes. Biomaterials. 2009; 30:4447–4456. [PubMed: 19535136]

17. Lindholt JS, Gottschalksen B, Johannesen N, Dueholm D, Ravn H, Christensen ED, et al. The Scandinavian Propaten((R)) trial- 1-year patency of PTFE vascular prostheses with heparinbonded luminal surfaces compared to ordinary pure PTFE vascular prostheses - a randomised clinical controlled multi-centre trial. Eur J Vasc Endovasc Surg. 2011; 41:668–673. [PubMed: 21376643]

18. Dorigo W, Pulli R, Castelli P, Dorrucci V, Ferilli F, De Blasis G, et al. A multicenter comparison between autologous saphenous vein and heparin-bonded expanded polytetrafluoroethylene (ePTFE) graft in the treatment of critical limb ischemia in diabetics. J Vasc Surg. 2011; 54:1332–1338. [PubMed: 21840151]

19. Hugl B, Nevelsteen A, Daenens K, Perez MA, Heider P, Railo M, et al. PEPE II--a multicenter study with an end-point heparin-bonded expanded polytetrafluoroethylene vascular graft for above and below knee by pass surgery: determinants of patency. J Cardiovasc Surg. 2009; 50:195–203. [PubMed: 19329916]

20. Kemp MM, Linhardt RJ. Heparin-based nanoparticles. Wiley Interdiscip Rev Nanomed Nanobiotechnol. 2010; 2:77–87. [PubMed: 20049832]

21. Kemp MM, Kumar A, Clement D, Ajayan P, Mousa S, Linhardt RJ. Hyaluronan- and heparin-reduced silver nanoparticles with antimicrobial properties. Nanomedicine (Lond). 2009; 4:421–429. [PubMed: 19505245]

22. Kemp MM, Kumar A, Mousa S, Park TJ, Ajayan P, Kubotera N, et al. Synthesis of gold and silver nanoparticles stabilized with glycosaminoglycans having distinctive biological activities. Biomacromolecules. 2009; 10:589–595. [PubMed: 19226107]

23. Murugesan S, Xie J, Linhardt RJ. Immobilization of heparin: approaches and applications. Curr Top Med Chem. 2008; 8:80–100. [PubMed: 18289079]

24. Tornoe CW, Christensen C, Meldal M. Peptidotriazoles on solid phase: [1,2,3]-triazoles by regiospecific copper(i)-catalyzed 1,3-dipolar cycloadditions of terminal alkynes to azides. J Org Chem. 2002; 67:3057–3064. [PubMed: 11975567]

25. Srinivasachari S, Fichter KM, Reineke TM. Polycationic beta-cyclodextrin “click clusters”: monodisperse and versatile scaffolds for nucleic acid delivery. J Am Chem Soc. 2008; 130:4618–4627. [PubMed: 18338883]

26. Iha RK, Wooley KL, Nystrom AM, Burke DJ, Kade MJ, Hawker CJ. Applications of orthogonal “click” chemistries in the synthesis of functional soft materials. Chem Rev. 2009; 109:5620–5686. [PubMed: 19905010]

27. Miao J, Pangule RC, Paskaleva EE, Hwang EE, Kane RS, Linhardt RJ, et al. Lysostaphin-functionalized cellulose fibers with antistaphylococcal activity for wound healing applications. Biomaterials. 2011; 32:9557–9567. [PubMed: 21959009]

28. Liang Y, Kiick KL. Heparin-functionalized polymeric biomaterials in tissue engineering and drug delivery applications. Acta Biomater. 2013

29. Born GV, Palinski W. Unusually high concentrations of sialic acids on the surface of vascular endothelia. Br J Exp Pathol. 1985; 66:543–549. [PubMed: 4063159]

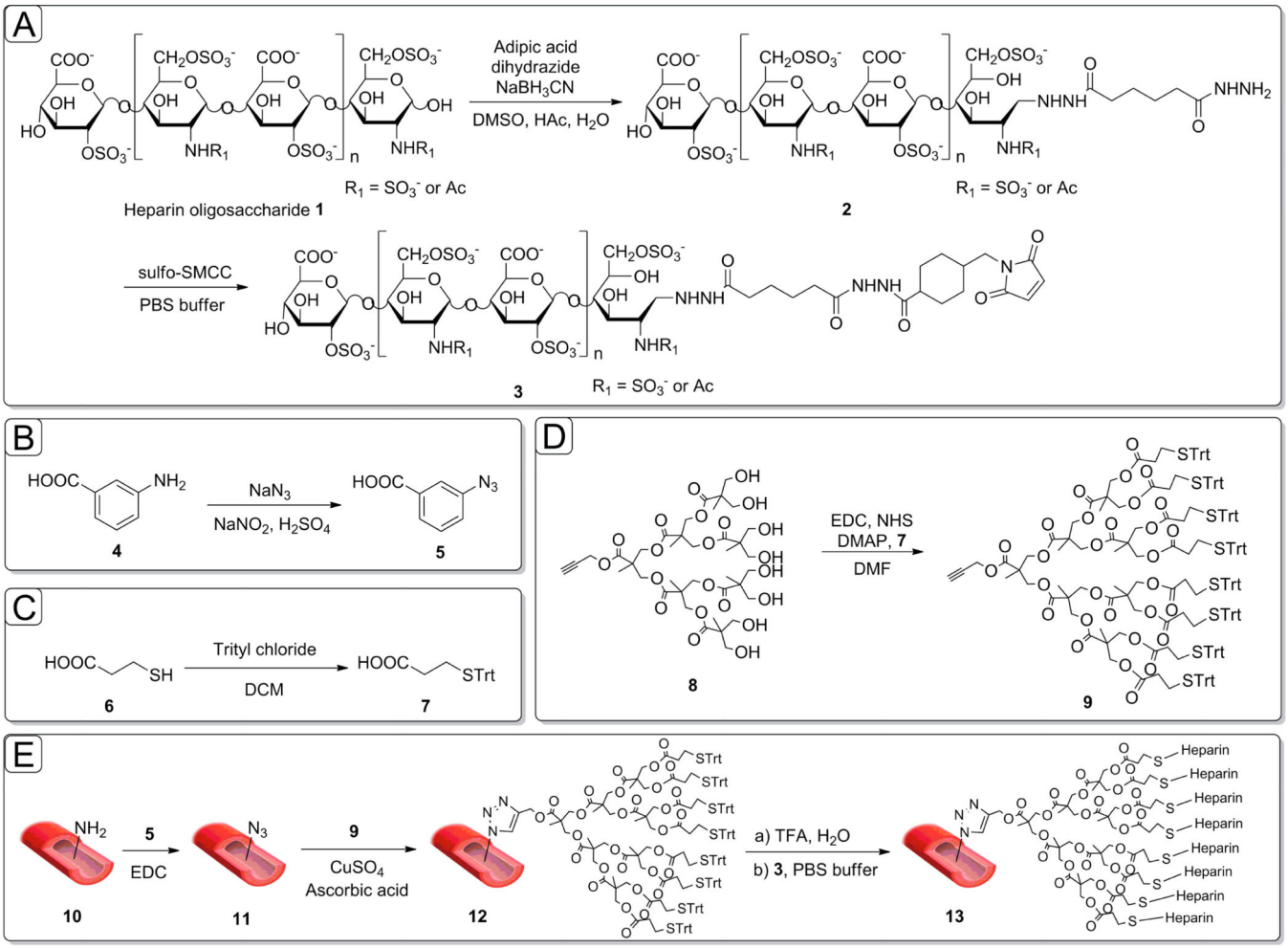

Figure 1.

Schematic description of the oriented heparin coating synthesis on decellularized aorta. A) The maleimide modification of heparin is described; B) & C) Modification of linear linkers for dendron coupling. D) Modification of dendron core. E) Amplification process on the amine groups of decellularized aortas through “clicked” dendrons and end-on oriented heparin coating of dendrons.

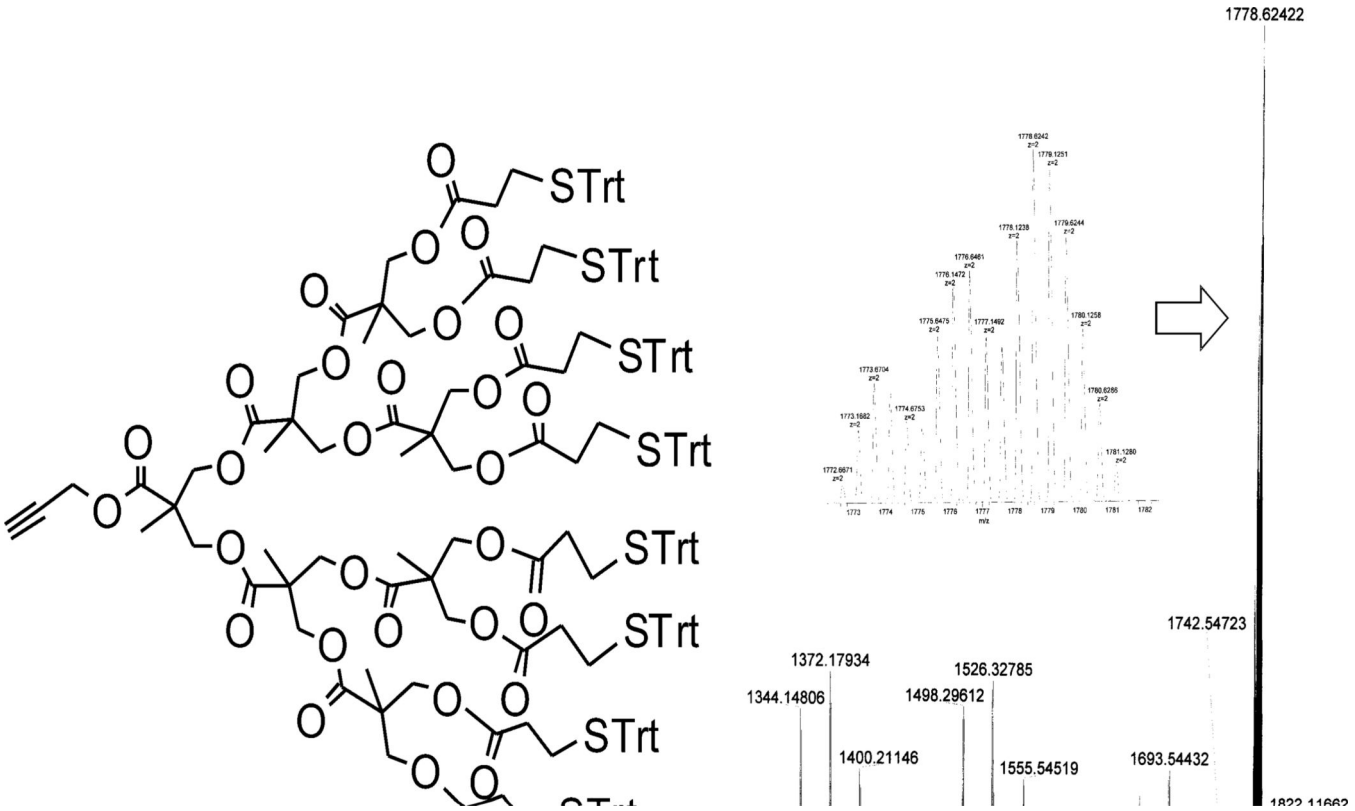

Figure 2.
MS characterization of dendron **9**.

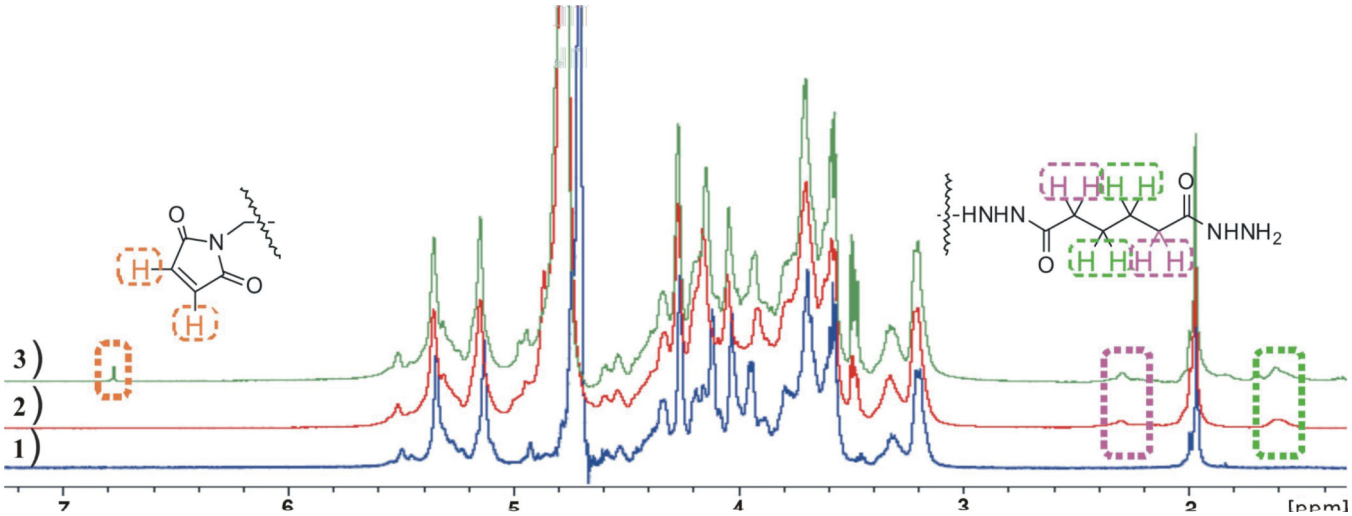

Figure 3.

^{1}H-NMR characterization of heparin modifications. The blue ^{1}H-NMR scan corresponds to unmodified heparin. The red ^{1}H-NMR scan corresponds to ADH-modified heparin. The green ^{1}H-NMR scan corresponds to the ADH-maleimide modified heparin. The signals for the maleamide protons are boxed in brown, and the ADH protons are boxed in green and purple. See Figure 1A for structures.

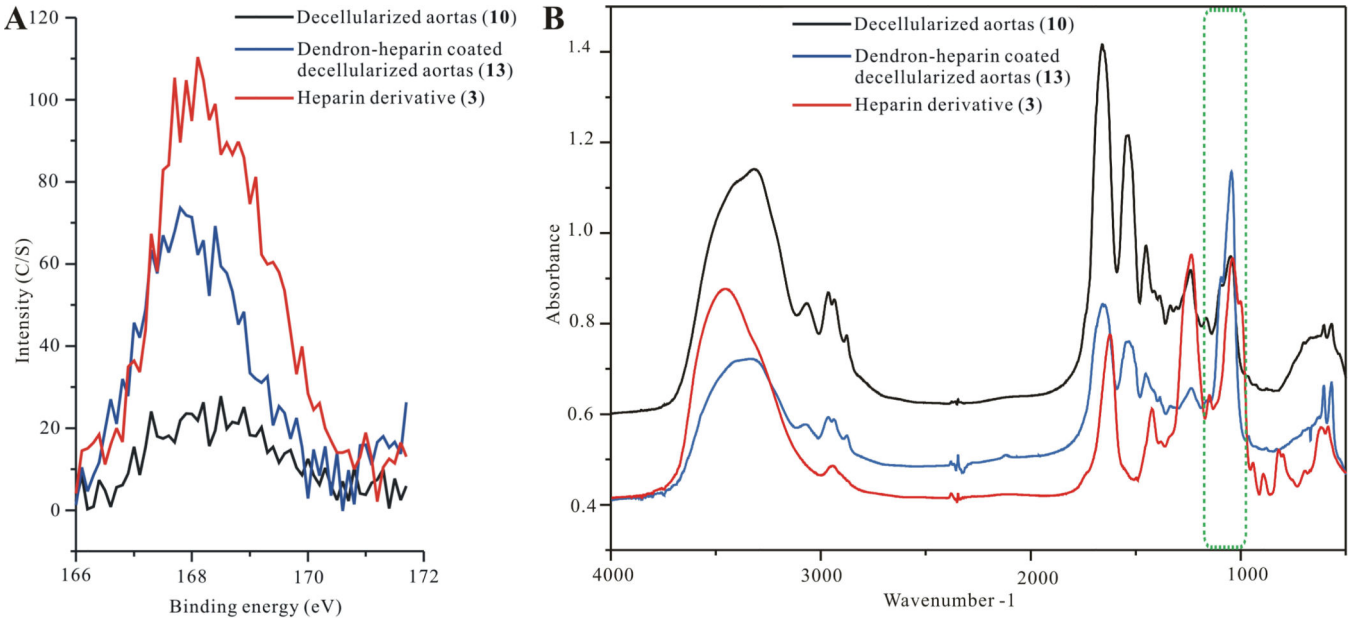

Figure 4.

A) XPS verification of heparin attachment on “click” coated decellularized aortas, B) FTIR verification of heparin attachment on “click” coated decellularized aortas. In both XPS and FTIR the modifications are color identified where the control untreated decellularized aortas are black; dendron coated decellularized aortas are blue; and dendron-heparin coated decellularized aortas are drawn in red.

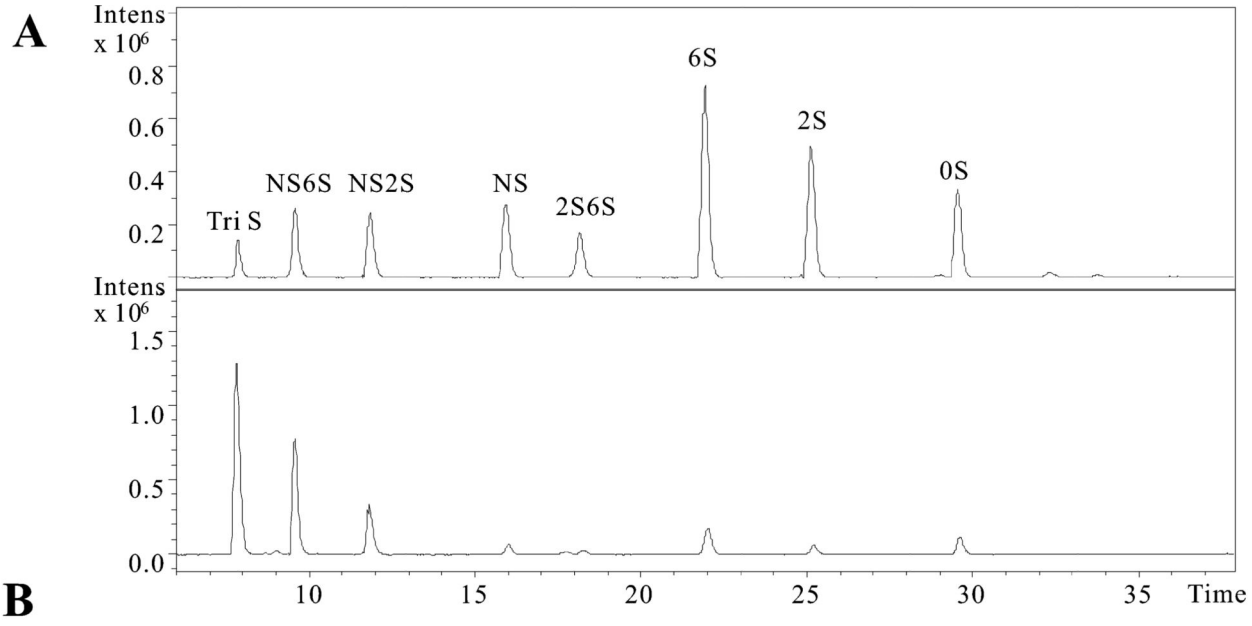

Sample	Heparin disaccharides composition (%)								Total amount
	ΔDi-TriS	ΔDi-NS6S	ΔDi-NS2S	ΔDi-NS	ΔDi-2S6S	ΔDi-6S	ΔDi-2S	ΔDi-0S	
decellularized aorta (1 cm^2)	68.18	17.11	7.81	1.37	1.02	1.59	0.87	2.04	16 μg

Figure 5.

Quantification of “click” immobilized heparin on decellularized aorta using disaccharide analysis relying on LC-MS. A) Extracted-ion chromatogram (EIC) of heparin/heparan sulfate disaccharide standards (top) and disaccharides released from “click” immobilized heparin on decellularized aorta sample (bottom). B) Table providing disaccharide composition as wt% of “click” immobilized heparin on decellularized aorta calculated from data shown in panel A.

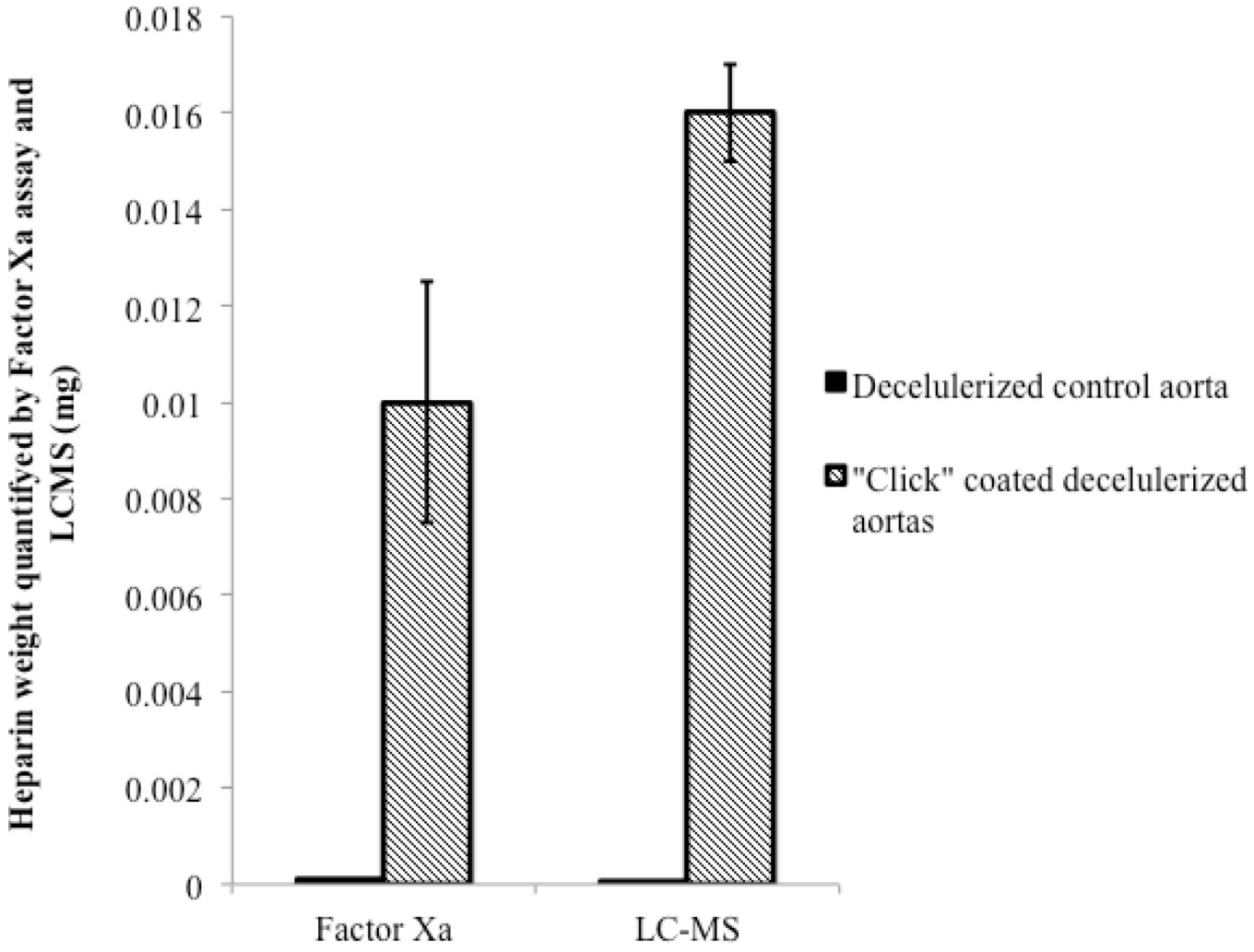

Figure 6.
Estimated functional heparin amount present on control untreated decellularized aortas and click-coated decellularized aortas as per the FXa assay.

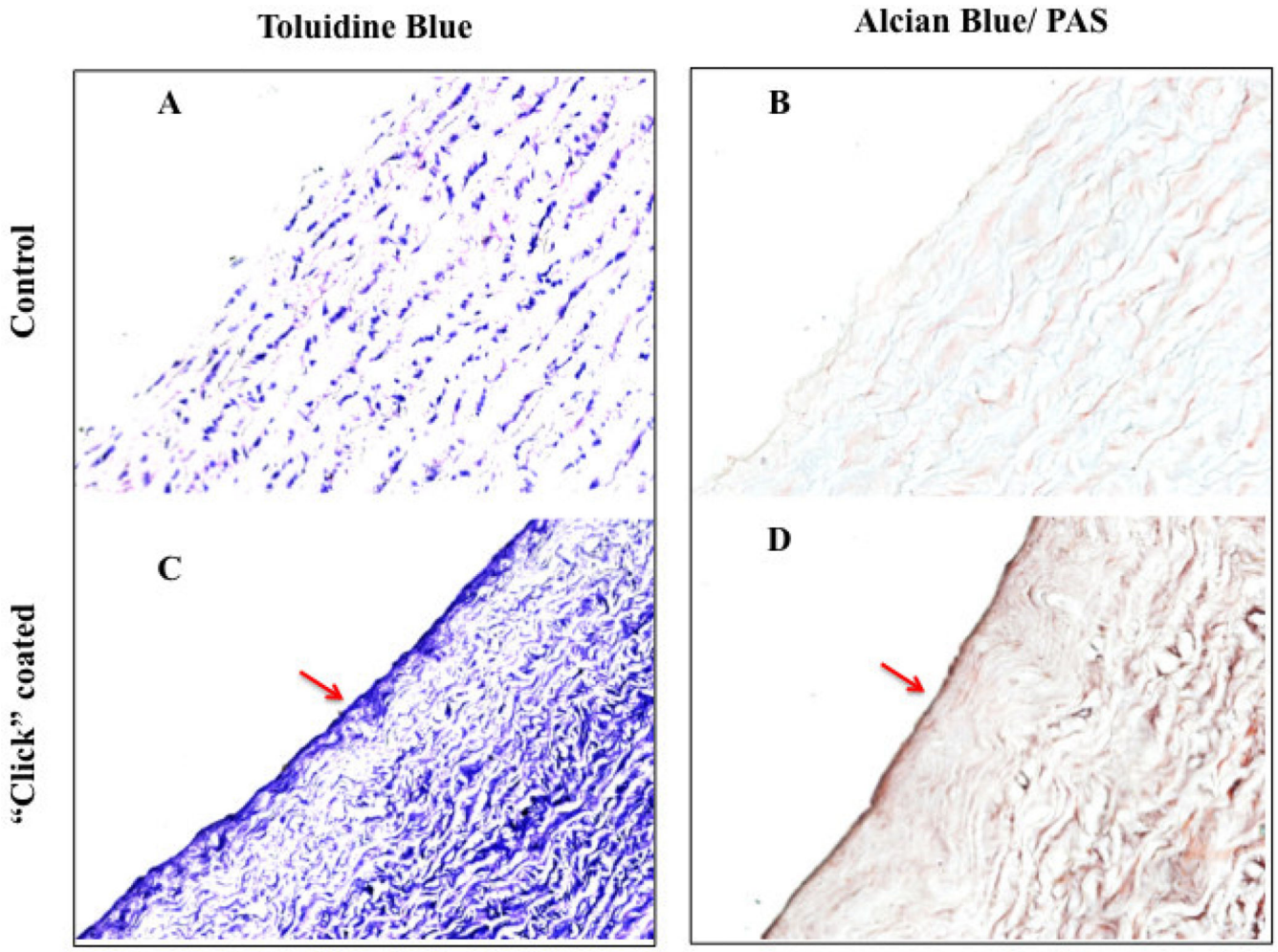

Figure 7.

Histology of control and click-coated decellularized aorta. Stains from left to right: Toluidine Blue and Alcian Blue/ PAS. Coating is visible with both dyes as a continuous layer covering the exposed collagen present in decellularized aorta (images C and D)

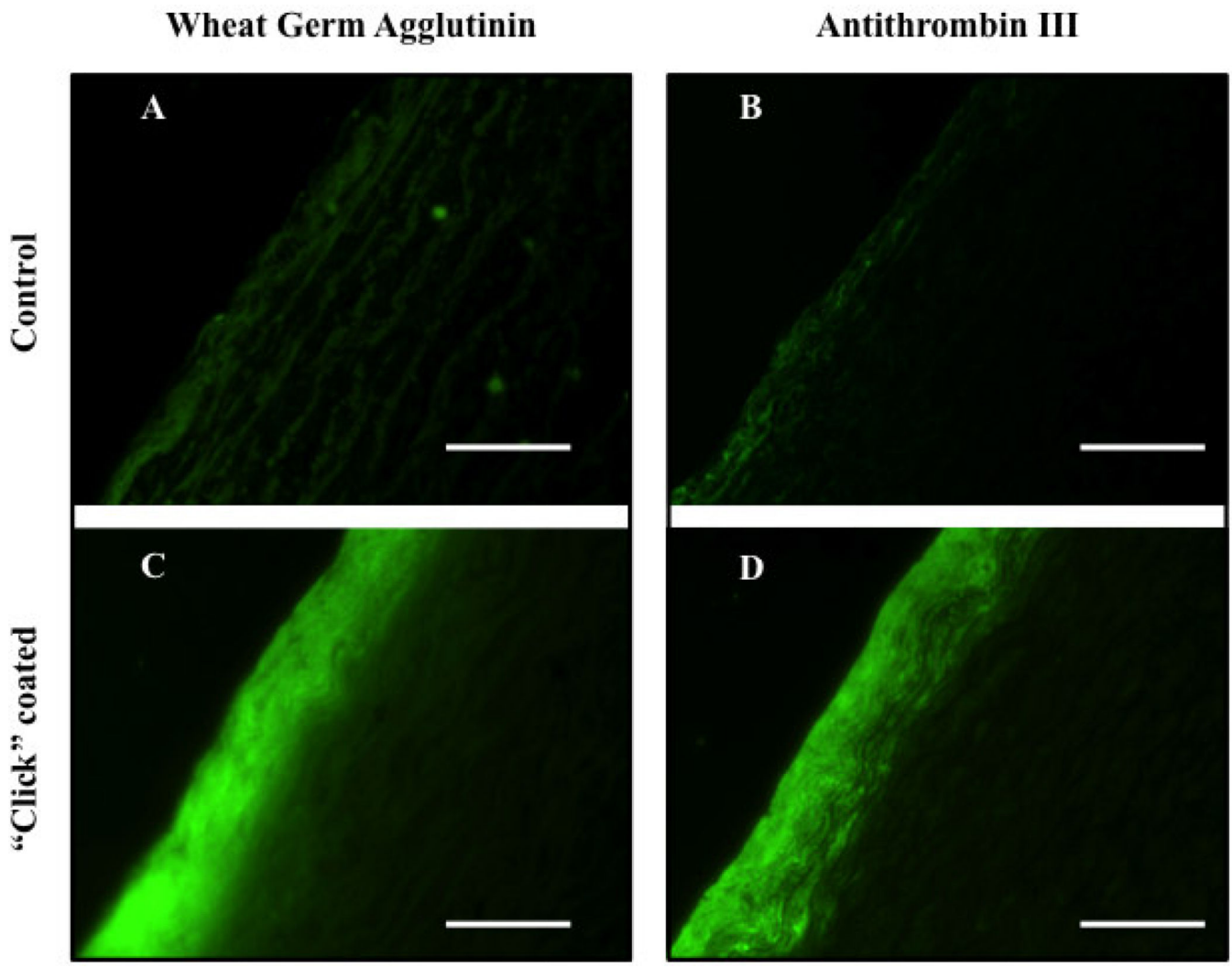

Figure 8.

Fluorescently labeled control and click-coated decellularized aorta imaged on 5μm thick slices. Coating is visible with both anti-wheat germ agglutinin-FITC antibody and ATIII-FITC staining as a continuous layer (images C and D). The decellularized aorta (control) shows a faint non-specific background absorbance on both stains.

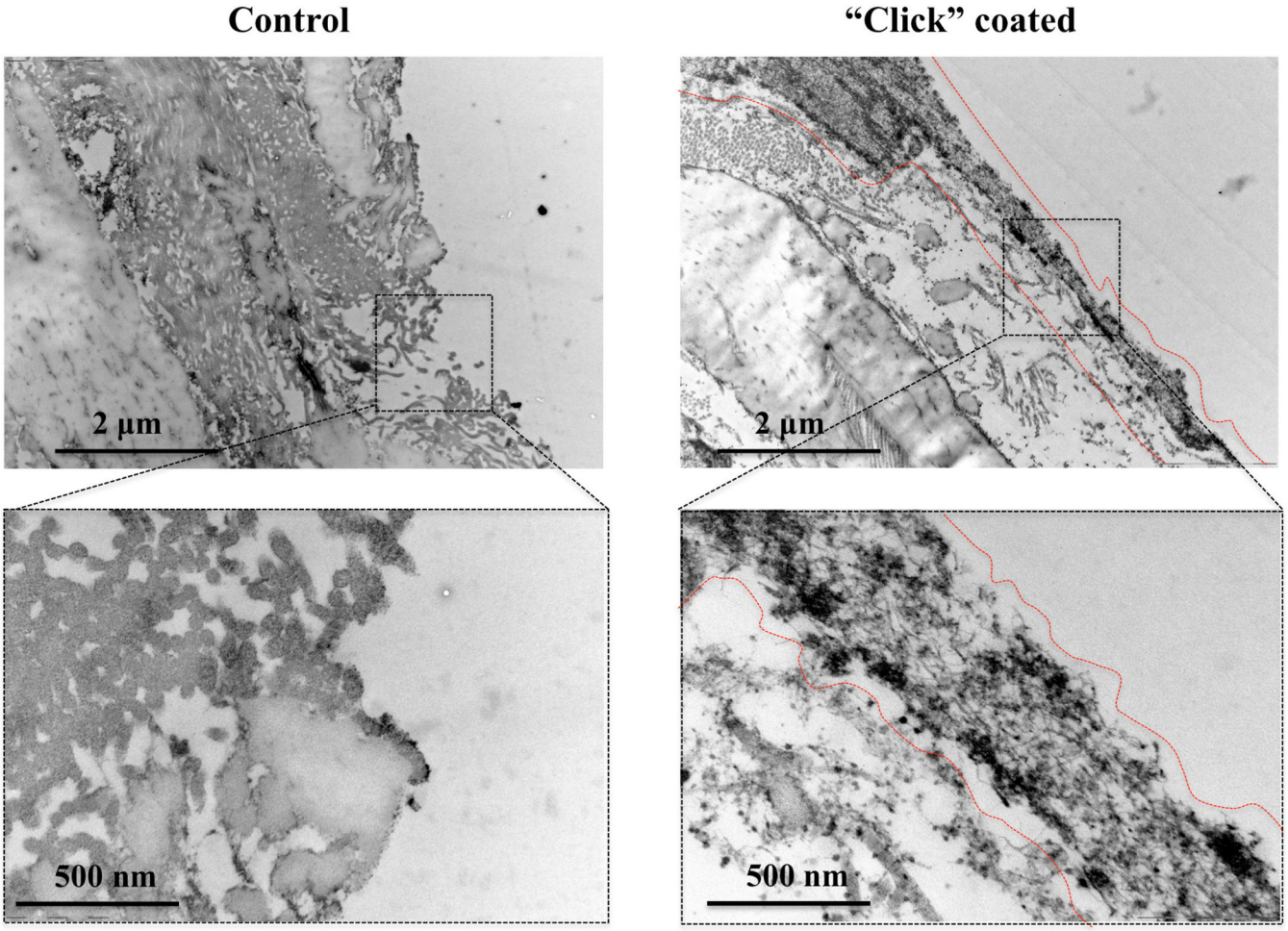

Figure 9.

Transmission Electron Microscopy (TEM) images of control decellularized aortas (left-hand panel) where elastin and mostly collagen fibers are exposed to the lumen; and on “click” heparin-coated decellularized aortas (right-hand panel) the 500 nm thick coating layer is shielding the otherwise exposed collagen.

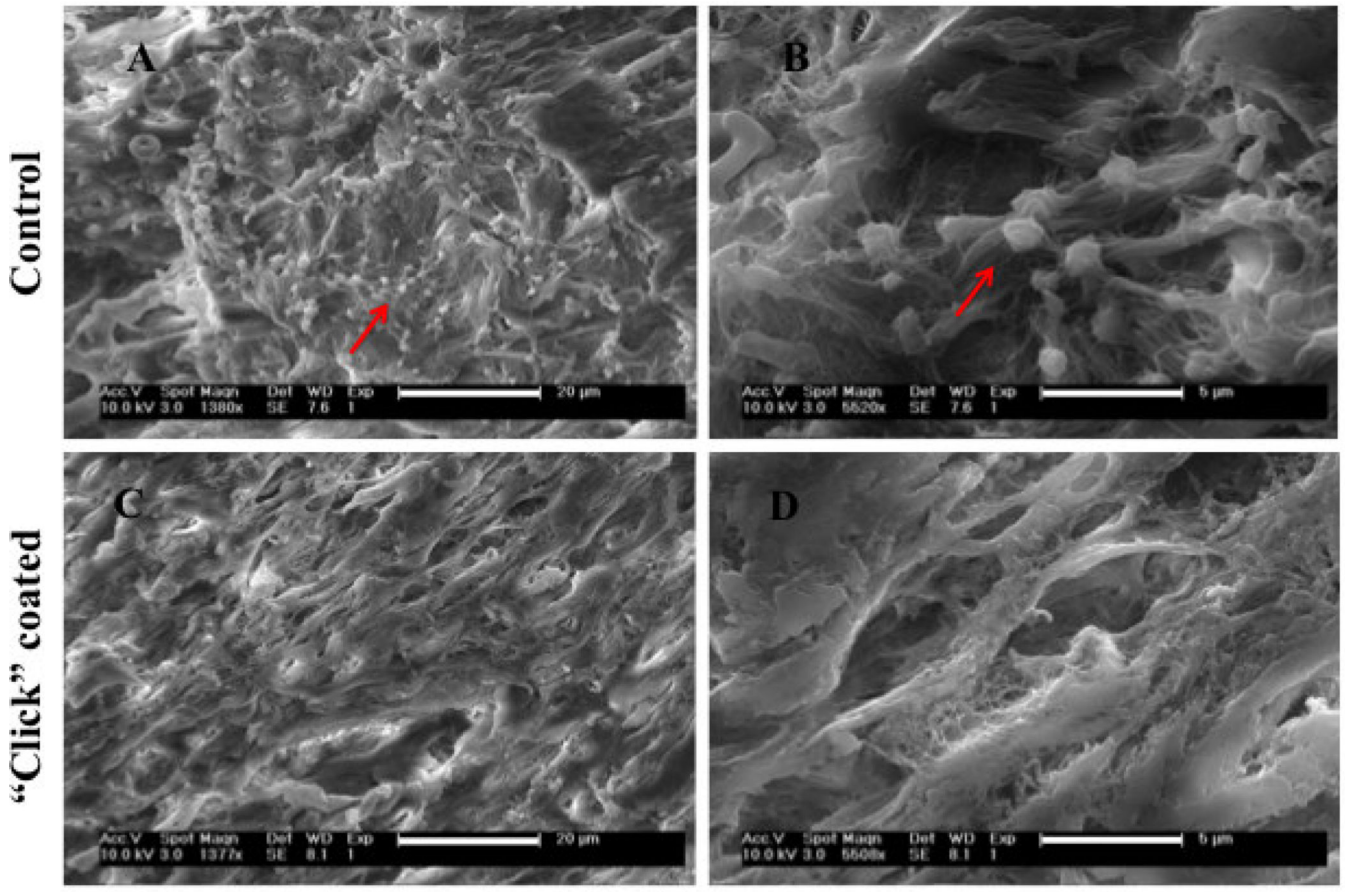

Figure 10.

Scanning Electron Micrograph of freshly isolated platelets incubated on control decellularized aortas (images A and B where platelets are identified by arrows) and on "click" heparin-coated decellularized aortas (images C and D showing the lack of platelets adhesion)

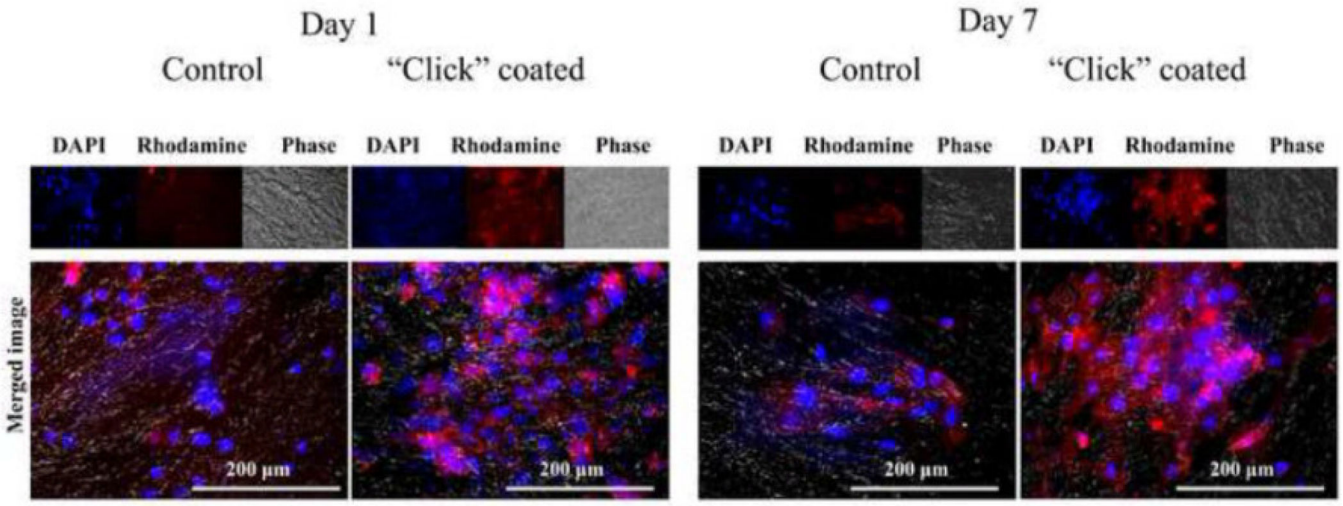

Figure 11.

Human Umbilical Vein Endothelial Cells (HUVECs) initial adhesion (Day 1) and growth (Day 7) on control decellularized aortas and "click" heparin-coated decellularized aortas visualized with Rhodaminephalloidin (red) and DAPI (blue).

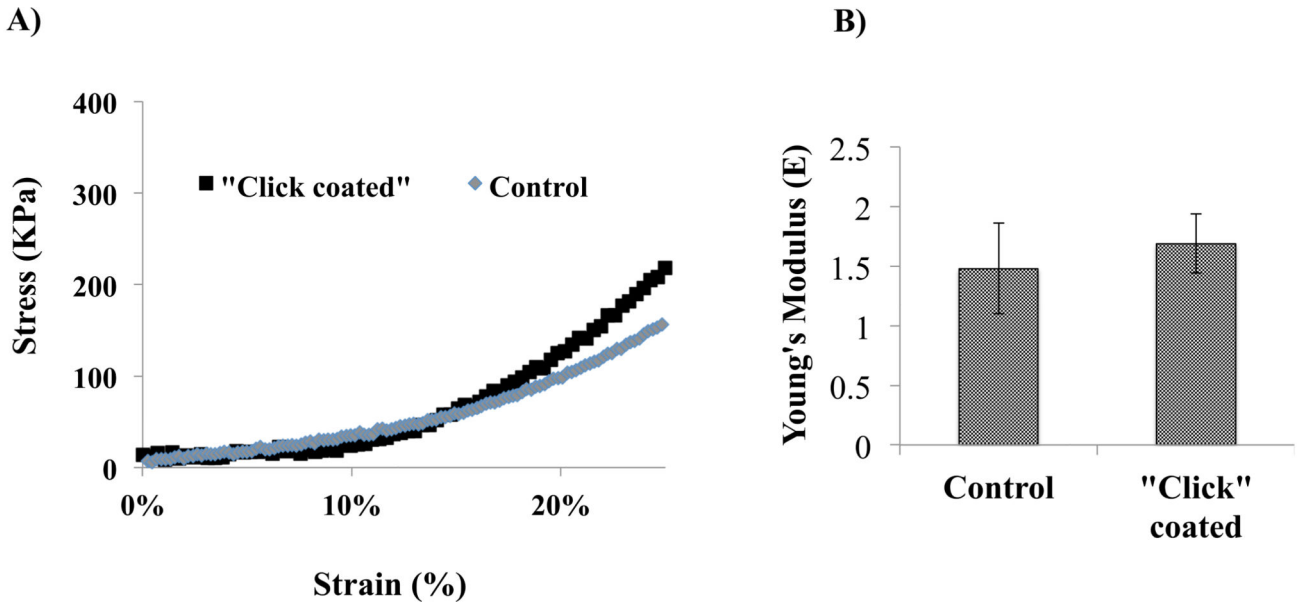

Figure 12.

Effects of “click” heparin coating on decellularized aortas mechanics. A) Stress strain curves of control decellularized aortas and “click” heparin-coated decellularized aortas sections. B) Young’s Moduli (average ± standard deviation) of control decellularized aortas and “click” heparin-coated decellularized aortas (n=3, 4 respectively). * Indicates significance at $p \leq 0.05$.